Proceedings IRG Annual Meeting (ISSN 2000-8953)

IRG/WP 25-11083

THE INTERNATIONAL RESEARCH GROUP ON WOOD PROTECTION

Section 1 **Biology**

Probing nanoscale protection mechanisms with x-rays and neutrons

Nayomi Z Plaza[1*], Katie M Ohno[1], Joseph E Jakes[1], James B O'Sullivan[2] and Lin Yang[3]

[1] USDA Forest Service
Forest Products Laboratory
One Gifford Pinchot Dr.
Madison, WI, USA

[2] Argonne National Laboratory
Lemont, Illinois, USA

[3] Brookhaven National Laboratory
Upton, New York, USA

Paper prepared for the IRG56 Scientific Conference on Wood Protection
Yokohama, Japan
22 – 26 June, 2025

IRG SECRETARIAT
Drottning Kristinas v. 61B
SE-114 86 Stockholm
Sweden
www.irg-wp.com

Probing nanoscale protection mechanisms with x-rays and neutrons

Nayomi Z Plaza[1], Katie M Ohno[1], Joseph E Jakes[1], James B O'Sullivan[2] and Lin Yang[3]

[1] US Forest Products Laboratory, Madison, Wisconsin, USA, nayomi.plazarodriguez@usda.gov; katie.m.ohno@usda.gov; joseph.e.jakes@usda.gov

[2] Argonne National Laboratory, Lemont, Illinois, USA, osullivanj@anl.gov

[3] Brookhaven National Laboratory, Upton, New York, USA; lyang@bnl.gov

ABSTRACT

While it is known that exposing wood to high levels of moisture, fire, or decay agents such as fungi can be detrimental for its performance, what is often missing in literature is a holistic understanding of how wood nanostructure changes due to these exposures. This is of particular interest since treatments that are meant to impart resistance can alter these length scales and/or modify their hygroscopic behavior. Yet, our knowledge of how protection treatments, such as chemical modification, alter the wood nanostructure is limited. X-ray and neutron scattering techniques are uniquely suited to probe these questions but remain underutilized in wood research. Small angle scattering can be used to measure the extent of chemical infiltration in the cell walls as well as the nanoscale swelling, while wide-angle scattering can probe changes in the cellulose crystalline structure. By combining these techniques, key nanoscale features that correlate with wood macroscale properties have been identified. For instance, model degraded woods with diminished mechanical properties had increased nanoscale disorder and swelling, while decay resistant chemically modified woods had reduced nanoscale swelling, and nanoscale features that were resistant to fungal exposure. An overview of the techniques as well as perspectives on the opportunities for their use in future wood protection research will be provided.

Keywords: x-ray scattering, neutron scattering, elementary fibrils, chemical modification, decay resistance

1. INTRODUCTION

While it is widely known that decay of wood leads to considerable strength loss at early stages of degradation (Arango *et al.* 2021, Ibach *et al.* 2014), our fundamental understanding of how current wood protection treatments impart decay resistance is limited. Recent research has shown that changes in the wood nanostructure can help explain moisture and mechanical properties of degraded wood systems (Broda *et al.* 2025), thus improving our understanding of modification of wood nanostructure could help inspire new wood protection systems. Knowledge gaps in this area stem from two main factors: (1) studying wood nanostructure is challenging, and (2) most efforts to study wood biodegradation at the nanoscale have been focused on understanding biodegradation from a mimicry standpoint. Although studying wood nanostructure continues to be challenging due to the poor contrast between the wood polymers and the structural complexity of the wood cell wall, scattering-based techniques could help fill these knowledge gaps, particularly with regards to changes at the elementary fibril level.

Previous work using X-ray diffraction and wide-angle X-ray scattering (WAXS) have provided insights on how fungi degrade cellulose and impart changes to its crystalline structure (Howell *et*

al. 2009, Hastrup *et al.* 2012, Zhu *et al.* 2022). Similarly, small angle neutron scattering (SANS) and small angle x-ray scattering (SAXS) have been used to measure the packing of the elementary fibrils and the elementary fibril diameter in woods that have been degraded via enzymatic or non-enzymatic treatments (Goodell *et al.* 2017, Zhu *et al.* 2020), and chemical treatments (Zitting *et al.* 2024, Pingali *et al.* 2010, Broda *et al.* 2025). SANS and SAXS have also been used to study the effects of chemical infiltration in contemporary wood (Plaza *et al.* 2019, Penttilä *et al.* 2020, Chen *et al.* 2021) and as well as archaeological waterlogged treated woods (Plaza *et al.* 2025). Most recently, SAXS-based tomography has been used to visualize the effects of thermal degradation in the transverse plane of charred wood samples without the need for sectioning (Plaza *et al.* 2024), however, this technique has yet to be utilized to study fungal degradation or wood protection systems.

This manuscript summarizes the key considerations for using SANS and SAXS-based techniques to study modified and/or decayed wood material. The effects of degradation and/or chemical modification on scattering data and multi-modal images such as scattering-based tomography are also shown and discussed.

2. EXPERIMENTAL METHODS

In general, preparation of wood specimens for scattering measurements is minimal. However, instrument geometry and primary anatomical orientation of the wood sample with respect to the detectors must be carefully considered. Sample thickness can vary from 2 microns to 1mm depending on the technique. Typically, thicker samples are preferred for neutron scattering experiments or x-ray scattering experiments where a larger probed volume is desired. Thinner specimens can be used at synchrotron beamlines and are useful for studying individual wood cell wall layers. All data shown here was obtained from longitudinal sections that were cut from larger 1cm x 1cm x 1cm blocks using a razor blade.

Scattering data is collected in reciprocal space. The accessible length scales in each experiment are defined in terms of the wavevector q, which is determined from the incident wavelength λ, scattering angle θ as follows:

$$q = 4\pi\sin(2\theta)/\lambda \quad (1)$$

2.1 Small angle scattering

Small angle neutron scattering (SANS) data shown is from previous research (Ibach *et al.* 2022, Broda *et al.* 2025 and Plaza *et al.* 2025). These were taken from unmodified and chemically modified *Pinus* spp. exposed to *Gloeophyllum trabeum* (Pers.) Murrill isolate MAD-617-R for 12 weeks at 26.7 °C and 70% Relative Humidity (RH) per ASTM D1413 (ASTM, 1999, Ibach *et al*. 2002)*, Pinus sylvestris* L. exposed to *Coniophora puteana* (Schum.: Fr.) P. Karst. isolate BAM 112 (BAM Ebw. 15) for 8 weeks at 24 ± 1 °C and 70 ± 5 RH in Kole flask decay chambers (Broda *et al.* 2022; Broda *et al*. 2025), and 1000-year-old archaeological waterlogged oak (*Quercus robur* L.) excavated from the Wielkopolska Region, Poland (Plaza *et al*. 2025). All data was obtained at the Bio-SANS beamline at the Oak Ridge National Laboratory (Oak Ridge, Tennessee, USA) using the standard dual detector configuration, and titanium cells that allowed measurement of longitudinal wood sections (~0.7 – 0.8 mm thick) while immersed in D_2O for maximum contrast. Larger thicknesses would result in more attenuated scattering profiles with less pronounced small angle diffraction peaks. Small angle x-ray scattering (SAXS) data shown is from (Broda *et al.* 2025, and Plaza *et al.* 2025) and was obtained from dry longitudinal sections (~0.8mm thick) measured at room and temperature conditions. Data was collected at the Oak Ridge National

Laboratory using a Xeuss 3.0 by Xenocs (Grenoble, France) x-ray scattering system with a Ga metal jet source and a 0.5 mm spot size.

2.2 Multi-modal imaging

Radial-longitudinal sections (10 mm long with a 1.5 – 2mm square cross-section) were cut from 1cm cubes of *Pinus taeda* spp. that were exposed to the decay fungus *G. trabeum* (Pers.) Murrill isolate MAD-617-R in soil bottles following the American Wood Protection Association Standard E-10-22 (AWPA, 2022). Soil bottles were incubated at 27 ℃, 70% RH for up to 12 weeks. The blocks were removed after different exposure times (i.e. 2-week, 6-weeks, etc.), oven dried (60°) overnight and reconditioned at 27 ℃, 30% RH. Imaging specimens were cut so that they contained both earlywood and latewood sections within an exposed sample. Then, these specimens were measured using the structural scanning configuration (Yang *et al.* 2022) with a focused X-ray beam spot size of 5 microns at the 16ID LiX beamline at the National Synchrotron Light Source II at the Brookhaven National Laboratory (Upton, New York, USA). Tomographic reconstructions were performed based on small angle x-ray scattering (SAXS), wide-angle x-ray scattering (WAXS) and x-ray fluorescence (XRF). XRF allows to map the trace amounts of mid- to high-Z elements in the wood cell walls at the spatial resolution of the X-ray beam (Paunesku *et al.* 2006). Wood longitudinal sections were mounted so that the longitudinal axis was vertically oriented and perpendicular to the incident beam. To minimize self-absorption effects in the analyzed region, which was either adjacent or opposite the feeder strip, samples were first tapered to form a thin tip. Measurements were then taken at various locations away from the tip to test for self-absorption effects in the fluoresced photons. Tomographic reconstructions based on the scattering contrast were performed using tomopy libraries (Gürsoy *et al*. 2014) as outlined in (Yang 2024). The following q-ranges were used to define the structural maps: 0.08- 0.18 A^{-1} for SAXS, and 1.52 - 1.58 A^{-1} for the WAXS crystalline signal (based on the 200-diffraction peak) and 1.26 - 1.32 A^{-1} for the amorphous component. A crystallinity index map was calculated by subtracting the amorphous signal from the crystalline map and then dividing it by the total crystalline signal. Fluorescence detectors allowed for simultaneous mapping of physiologically relevant elements: Fe, K, Ca, Mn and Zn across the wood cellular structure.

3. DEGRADATION EFFECTS ON SMALL ANGLE SCATTERING DATA

SANS and SAXS data from non-degraded and degraded wood samples are shown in Fig 1 a. For non-degraded wood, the long-range order of the elementary fibrils in the cell wall gives rise to a small angle diffraction (q~0.15 A^{-1}). As moisture enters the microfibrils the peak position shifts towards lower q as they swell (Plaza *et al.* 2016). The diffraction peak is much more pronounced in SANS data compared to SAXS because neutrons have higher contrast than x-rays. As the wood polymers are targeted by the decaying organism, the long-range order of the elementary fibrils, which gives rise to the small angle diffraction peak, is lost, and eventually the peak becomes indistinguishable. Chemically modifying wood can change wood nanostructure and the water accessibility of microfibrils. The effects of chemical modification (closed symbols) and subsequent fungal exposure (open symbols) on SANS data is shown in Fig 1b from Ibach *et al.* 2022. Chemically modified woods that suffered little weight loss due to a 12-week exposure to *G. trabeum* still contained the small angle diffraction peak due to water entering spaces between the elementary fibrils, albeit its intensity is less than chemically modified wood that had not been exposed to *G. trabeum*. Whereas chemically modified wood that was not resistant to *G. trabeum* lost this characteristic feature. Thus, chemical modifications that provided decay resistance also protected the wood nanostructure, particularly at the elementary fibril level.

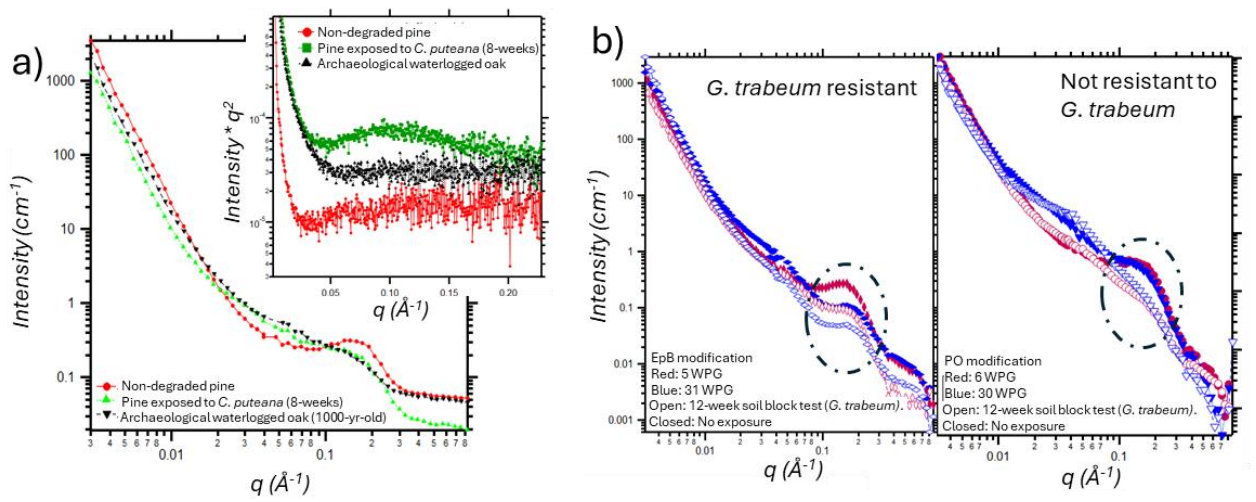

Figure 1: Effects of degradation on SANS data from (a) unmodified southern pine and (b) chemically modified southern pine showing that *G. trabeum* resistant samples still contain the SANS peak whereas non-resistant samples do not (shown in dashed oval). Effects of degradation on SAXS data from unmodified southern pine is shown in inset of (a). Data from scots pine exposed to *C. puteana* for 8-weeks (~40% mass loss) is from Broda *et al.* 2025, and archaeological waterlogged oak (~10% mass loss) is from Plaza *et al.* 2025. SANS data from southern pine modified with epoxybutene (EpB) (left side of (b)) or propylene oxide (PO) (right side of (b)) is from Ibach *et al.* 2022.

From the position (q_{pk}) of the small angle diffraction peak, we can obtain the elementary fibril spacing (EF) as:

$$EF = 2\pi/q_{pk} \quad (2)$$

The effects of chemical modification (as weight percentage gain (WPG) due to modification) and mass loss due to fungal exposure in a soil-block test are shown in Figure 2. Ibach *et al*. 2022, showed that increasing the WPG lowered EF (Fig. 2a). As wood is degraded EF increases, and the amount of swelling exceeds that of non-degraded unmodified wood. The chemical modifications most effective at imparting decay resistance reduce the amount of swelling at the elementary fibril level and lower the EF to values that are comparable to unmodified wood samples conditioned at 25 - 40% RH (Plaza *et al.* 2016).

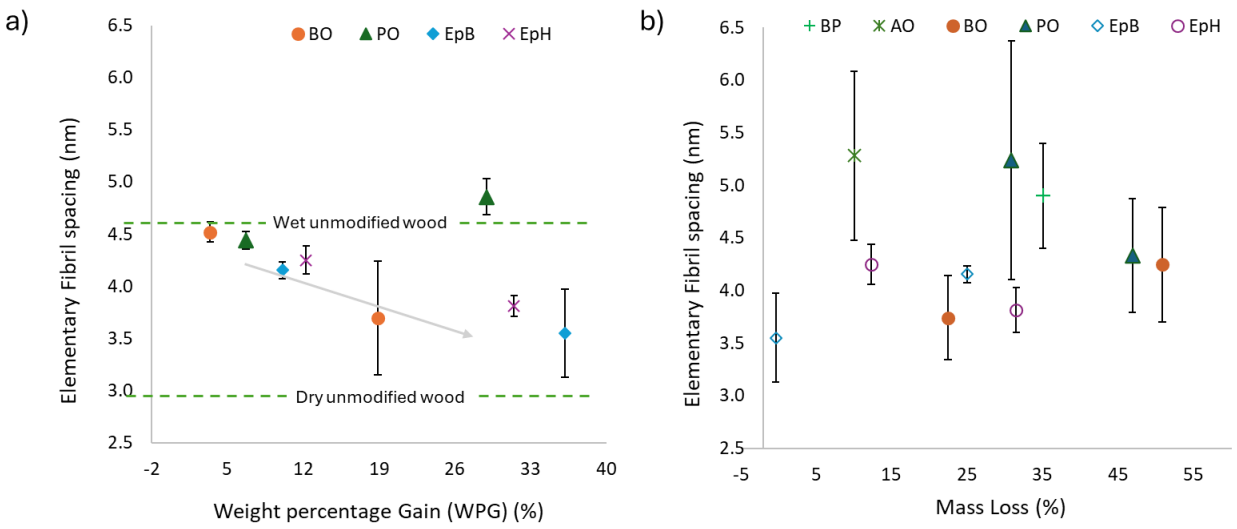

Figure 2: Effects of (a) chemical modification and (b) degradation on the elementary fibril spacing of chemically modified woods fully immersed in heavy water. Data for southern pine modified with butylene oxide (BO), propylene oxide (PO), epoxybutene (EpB) and epichlorohydrin (EpH) with and without 12-week exposure to *G. trabeum* is from Ibach *et al.* 2022. Data for degraded scots pine (BP) caused by fungal exposure to *C. puteana* and archaeological waterlogged oak (AO) is from Broda *et al.* 2025 and Plaza *et al.* 2025, respectively.

4. ASSESING DEGRADATION WITH MULTI-MODAL IMAGING

Tomographic maps from the Fe XRF as well as the scattering contrast at the elementary fibril level and the cellulose crystalline structure are shown in Figure 3 for a non-degraded wood sample (left) and for a sample that had been exposed to *G. trabeum* for 6-weeks (right) corresponding to approximately 26% mass loss. Fe maps were included because Fe is generated via a chelator mediated Fenton reaction and is one of the main non-enzymatic decay mechanisms used by *G. trabeum* (Arantes and Goodell 2014). The earlywood and latewood regions are clearly visible in the SAXS maps, and a small decrease in intensity is observed due to degradation. Cellulose crystallinity decreases following the exposure but to different extents throughout the sample. For the non-degraded control sample, the crystallinity index is uniform throughout both earlywood and latewood whereas in the degraded sample the earlywood is much less crystalline compared to the latewood. While a general loss in crystallinity following brown rot exposure has been observed previously (Howell *et al.* 2009, Hastrup *et al.* 2012), the heterogeneity observed in this work would likely be missed in traditional x-ray diffraction experiments such as powder diffraction. In the degraded sample, the concentration of Fe in the cell wall increases throughout the sample, which is consistent with previous XFM experiments (Kirker *et al.* 2017, Zelinka *et al.* 2019). By utilizing multi-modal imaging, we were able to visualize distributions of elementary fibril scattering, cellulose crystallinity, and ion movement in wood exposed to *G. trabeum*. This was one of the first attempts to use this type of imaging to better understand fungal decay as it progresses through untreated wood.

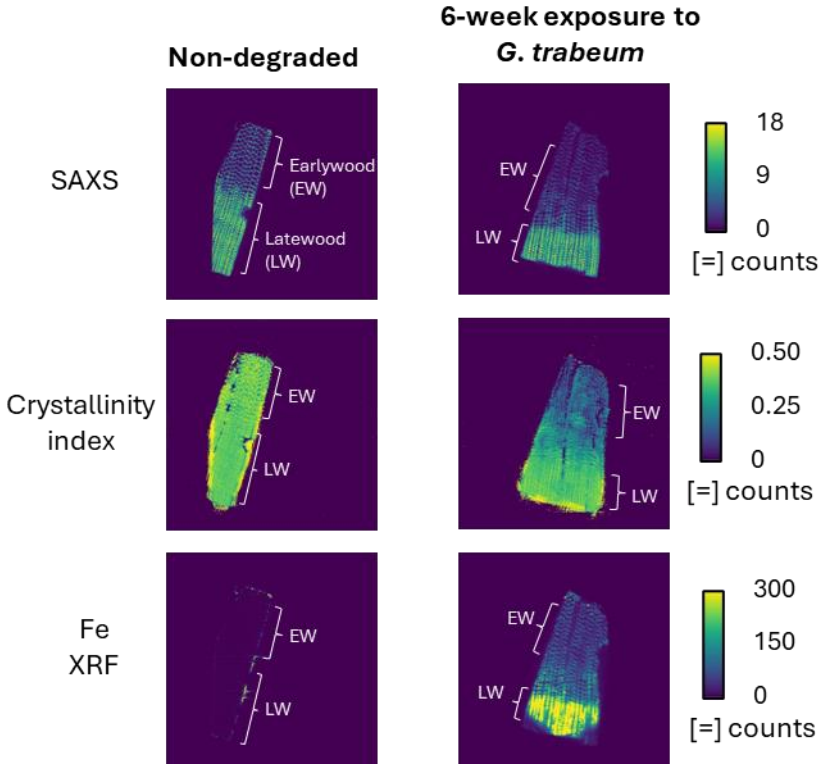

Figure 3: Effects of exposure to the brown rot decay fungus *G. trabeum* on the tomographic maps based on the scattering from elementary fibrils (SAXS), cellulose crystallinity index and the x-ray fluorescence (XRF) of Fe ions in the transverse cellular structure.

5. SUMMARY AND OUTLOOK

Scattering-based techniques have proven to be useful to study nanoscale swelling and degradation in wood due to chemical treatments and/or fungal exposure. Chemical modifications that impart decay resistance can protect wood nanostructure and reduce swelling at the elementary fibril level. Yet, more experiments exploring the temporal changes associated with chemical modification and fungal exposure are still needed to identify other mechanisms associated with improved decay resistance. By combining x-ray fluorescence with scattering-based tomography we can gain a more complete understanding of how degradation imparts changes in wood's hierarchical structure and distribution of chemicals in the wood cell walls. Thus, multimodal imaging offers a unique opportunity for future studies aiming to understand decay protection mechanisms in chemically modified woods.

6. ACKNOWLEDGEMENT

This research was supported in part by the U.S. Department of Agriculture, Forest Service. The authors would like to acknowledge the use of 16ID-LiX at NSLS. The LiX beamline, which is part of the Center for BioMolecular Structure (CBMS), which is primarily supported by the National Institutes of Health, National Institute of General Medical Sciences (NIGMS) through a P30 Grant (P30GM133893), and by the DOE Office of Biological and Environmental Research (KP1605010). LiX also received additional support from NIH Grant S10 OD012331. As part of NSLS-II, a national user facility at Brookhaven National Laboratory, work performed at the

CBMS is supported in part by the U.S. Department of Energy, Office of Science, Office of Basic Energy Sciences Program under contract number DE-SC0012704. Multi-modal imaging results in this report are derived from work performed through the eBERlight program, funded by the U.S. Department of Energy, Office of Biological and Environmental Research, by the U.S. DOE, Office of Basic Energy Sciences, under Contract No. DE-AC02-06CH11357. A portion of this research was performed on a project award (10.46936/fics.proj.2023.60858/60008907) under the FICUS program and used resources at the DOE Joint Genome Institute and the Environmental Molecular Sciences Laboratory, which are DOE Office of Science User Facilities. Both facilities are sponsored by the Biological and Environmental Research program and operated under Contract Nos. DE-AC02-05CH11231 (JGI) and DE-AC05-76RL01830 (EMSL). The authors would also like to acknowledge Amy Bishell from the Forest Products Laboratory for her technical assistance in the laboratory.

6. REFERENCES

American Wood Protection Association (2022): Standard methods of testing wood preservatives by laboratory soil-block cultures. Standard E10-18. Book of Standards. American Wood-Preservers Association, Birmingham, AL, pp. 418-428.

Arango, R, Lebow, S T, Glaeser, J A (2021): Chapter 14: Biodeterioration of wood. In: Wood handbook – wood as an engineering material. General Technical Report FPL-GTR-282. Madison, WI: U.S. Department of Agriculture, Forest Service, Forest Products Laboratory. 19 pp.

Arantes, V, Goodell, B (2014): Current Understanding of Brown-Rot Fungal Biodegradation Mechanisms: A Review. *Deterioration and Protection of Sustainable Biomaterials*, 3-21. https://doi.org/10.1021/bk-2014-1158.ch001

ASTM (1999): ASTM standard method of testing wood preservatives by laboratory soil-block cultures. American Society Testing Materials Des. 9:1413.

Broda, M, Plaza, N Z, Jakes, J E, Baez, C, Pingali, S V, Bras, W (2025): Effect of alkali treatment and fungal degradation on the nanostructure and cellulose arrangement in Scots pine cell walls – A neutron and X-ray scattering study. *Carbohydrate Polymers*, **347**, 122733. https://doi.org/10.1016/j.carbpol.2024.122733

Broda, M, Popescu, C, Curling, S, Timpu, D, Ormondroyd, G A (2022): Effects of biological and chemical degradation on the properties of scots pine wood – part I: chemical composition and microstructure of the cell wall. *Materials*, **15**(7), 2348. https://doi.org/10.3390/ma15072348

Chen, P, Li, Y, Nishiyama, Y, Pingali, S V, O'Neill, H M, Zhang, Q, Berglund, L A (2021): Small Angle Neutron Scattering Shows Nanoscale PMMA Distribution in Transparent Wood Biocomposites. *Nano Letters*, **21**(7), 2883-2890. https://doi.org/10.1021/acs.nanolett.0c05038

Goodell, B, Zhu, Y, Kim, S, Kafle, K, Eastwood, D, Daniel, G, Jellison, J, Yoshida, M, Groom, L, Pingali, S V, O'Neill, H, O'Neill, H (2017): Modification of the nanostructure of lignocellulose cell walls via a non-enzymatic lignocellulose deconstruction system in brown rot wood-decay fungi. *Biotechnology for Biofuels*, **10**(1), 179. https://doi.org/10.1186/s13068-017-0865-2

Gürsoy D, De Carlo F, Xiao X, & Jacobsen C. (2014). Tomopy: a framework for the analysis of synchrotron tomographic data. Journal of Synchrotron Radiation, 21(5):1188–1193

Hastrup, A C S, Howell, C, Larsen, F H, Sathitsuksanoh, N, Goodell, B, Jellison, J (2012): Differences in crystalline cellulose modification due to degradation by brown and white rot fungi. *Fungal Biology*, **116**(10), 1052-1063. https://doi.org/10.1016/j.funbio.2012.07.009

Howell, C, Steenkjær Hastrup, A C, Goodell, B, Jellison, J (2009): Temporal changes in wood crystalline cellulose during degradation by brown rot fungi. *International Biodeterioration and Biodegradation,* **63**(4), 414-419. https://doi.org/10.1016/j.ibiod.2008.11.009

Ibach, R E, Plaza, N Z, Pingali, S V (2022): Small Angle Neutron Scattering Reveals Wood Nanostructural Features in Decay Resistant Chemically Modified Wood. *Frontiers in Forests and Global Change*, **4**(January), 1-11. https://doi.org/10.3389/ffgc.2021.814086

Ibach, R E, Lebow, S, Patricia, K (2014): *Strength loss in decayed wood*. In: the McGraw-Hill Encyclopedia of Science & Technology, 2014, pp. 368-371.

Kirker, G, Zelinka, S, Gleber, S C, Vine, D, Finney, L, Chen, S, Hong, Y P, Uyarte, O, Vogt, S, Jellison, J, Goodell, B, Jakes, J E (2017): Synchrotron-based X-ray fluorescence microscopy enables multiscale spatial visualization of ions involved in fungal lignocellulose deconstruction. *Scientific Reports*, **7**. https://doi.org/10.1038/srep41798

Paunesku, T, Vogt, S, Maser, J, Lai, B, Woloschak, G (2006): X-ray fluorescence microprobe imaging in biology and medicine. *Journal of Cellular Biochemistry*, **99**, 1489-1502. https://doi.org/10.1002/jcb.21047

Penttilä, P A, Altgen, M, Awais, M, Österberg, M, Rautkari, L, Schweins, R (2020): Bundling of cellulose microfibrils in native and polyethylene glycol-containing wood cell walls revealed by small-angle neutron scattering. *Scientific Reports*, **10**(1), 1-9. https://doi.org/10.1038/s41598-020-77755-y

Pingali, S V, Urban, V S, Heller, W T, McGaughey, J, O'Neill, H, Foston, M, Myles, D A, Ragauskas, A, Evans, B R (2010): Breakdown of Cell Wall Nanostructure in Dilute Acid Pretreated Biomass. *Biomacromolecules*, **11**(9), 2329-2335. https://doi.org/10.1021/bm100455h

Plaza, N Z, Pingali, S V, Broda, M (2025): The effect of organosilicon compounds on the nanostructure of waterlogged archeological oak studied by neutron and X-ray scattering. *Journal of Cultural Heritage*, **71**, 203-210. https://doi.org/10.1016/j.culher.2024.11.021

Plaza, N Z, Pingali, S V, Ibach, R E (2022): Nanostructural Changes Correlated to Decay Resistance of Chemically Modified Wood Fibers. *Fibers*, **10**(5), 1-14. https://doi.org/10.3390/fib10050040

Yang, L, Liu, J, Chodankar, S, Antonelli, S, DiFabio, J (2022.): Scanning structural mapping at the Life Science X-ray Scattering Beamline. *Journal of Synchrotron Radiation,* **29**, 540-548.

Yang, L (2024): X-ray scattering based scanning tomography for imaging and structural characterization of cellulose in plants. *Journal of Synchrotron Radiation*, **31**(Pt 4), 936-947. https://doi.org/10.1107/S1600577524004387

Zelinka, S L, Jakes, J E, Tang, J, Ohno, K, Bishell, A, Finney, L, Maxey, E R, Vogt, S, Kirker, G T (2019): Fungal–copper interactions in wood examined with large field of view synchrotron–

based x–ray fluorescence microscopy. *Wood Material Science and Engineering*, **14**(3), 174-184. https://doi.org/10.1080/17480272.2018.1458049

Zhu, Y, Plaza, N, Kojima, Y, Yoshida, M, Zhang, J, Jellison, J, Pingali, S V, O'Neill, H, Goodell, B (2020): Nanostructural Analysis of Enzymatic and Non-enzymatic Brown Rot Fungal Deconstruction of the Lignocellulose Cell Wall†. *Frontiers in Microbiology*, **11**(June), 1-14. https://doi.org/10.3389/fmicb.2020.01389

Zhu, Y, Li, W, Meng, D, Li, X, Goodell, B (2022): Non-enzymatic modification of the crystalline structure and chemistry of Masson pine in brown-rot decay. *Carbohydrate Polymers*, **286**(2), 119242. https://doi.org/10.1016/j.carbpol.2022.119242

Zitting, A, Paajanen, A, Altgen, M, Rautkari, L, Penttilä, P A (2024): Role of Lignin in Moisture Interactions of Cellulose Microfibril Structures in Wood. *Small Structures*, 5(12), 1-14. https://doi.org/10.1002/sstr.202400167